

From the Square Lattice to the Checkerboard Lattice : Spin Wave and Large-n limit Analysis

Benjamin Canals*

*Laboratoire Louis Néel, CNRS, 25 avenue des Martyrs,
Boite Postale 166, 38042 Grenoble Cedex 9, France*

(Dated: December 2, 2024)

Within a spin wave analysis and a fermionic large- n limit, it is shown that the antiferromagnetic Heisenberg model on the checkerboard lattice may have different ground states, depending on the spin size S . Through an additional exchange interaction that corresponds to an inter-tetrahedra coupling, the stability of the Néel state has been explored for all cases from the square lattice to the isotropic checkerboard lattice. Away from the isotropic limit and within the linear spin wave approximation, it is shown that there exists a critical coupling for which the local magnetization of the Néel state vanishes for any value of the spin S . On the other hand, using the Dyson-Maleev approximation, this result is valid only in the case $S = \frac{1}{2}$ and the limit between a stable and an unstable Néel state is at $S = 1$. For $S = \frac{1}{2}$, the fermionic large- n limit suggests that the ground state is a valence bond solid build with disconnected 4-spins singlets. This analysis indicates that for low spin and in the isotropic limit, the checkerboard antiferromagnet may be close to an instability between an ordered $S = 0$ ground state and a magnetized ground state.

PACS numbers: 75.10.Jm, 75.30.Ds, 75.50.Ee

I. INTRODUCTION

In one dimension (1D) the ground state of the Heisenberg antiferromagnet may be quasi-ordered or disordered, depending on the spin parity S^1 . When S is an integer, and in particular, when $S = 1$, the ground state corresponds to a magnetically disordered state where spin-spin correlation functions (CFs) exponentially decay with distance and with total spin $S_t = 0$. This state is called a quantum spin liquid (QSL) as the spin-spin CFs are equivalent to the density-density CFs in conventional liquids and because it has total spin $S = 0$ and no broken symmetry. This concept can be generalized to classical systems if the spins are considered as $O(3)$ vectors. The constraint $S = 0$ is then removed and the state is termed a classical spin liquid (CSL). Another notion for spin liquid ground states emerged from earlier studies by Wannier² and Houtappel³ and is related to geometrical frustration. In that case, it is the geometry of the underlying lattice that leads to magnetic disorder and not its dimensionality. Naturally, frustrated structures may exist not only for $D = 1$ and for over 50 years frustrated lattices have been examined in the search for disordered ground states in higher dimensions ($D = 2, 3$). One goal of this research into peculiar structures is the study of unconventional spectra, not covered by the Lieb and Mattis theorem⁴.

To date, two particular lattices have been considered as good candidates for spin liquid ground states : the kagomé lattice and the pyrochlore lattice. The first one is a two dimensional arrangement of corner sharing triangles, while the latter is a three dimensional structure of corner sharing tetrahedra. Both lattices have been theoretically investigated and it has been suggested that in the classical case, as well as in the quantum case, they possess spin liquid like ground states^{5,6,7,8}. Experimen-

tally, all systems that can be well described by the antiferromagnetic Heisenberg model on these lattices have been found to possess this spin liquid behavior or unconventional behaviors that can be ascribed in part to the underlying “theoretical” spin liquid ground state⁹. This suggests that both the elementary cells (triangle or tetrahedron) and the connectivity (corner sharing) are major ingredients for magnetic disorder. In this paper, we study such a lattice, where the elementary cell is a tetrahedron and where connectivity is corner sharing : the checkerboard lattice (see Fig. 1). This system is two dimensional and can be described as the two dimensional analog of the pyrochlore lattice : each atom possess locally the same environment. It has recently been proven that its quantum ground states are singlets¹⁰ for finite systems. The aim of this work is to test whether this conclusion may be valid for an infinite lattice. To do so we start away from the isotropic checkerboard limit, when diagonal bonds are weakened (see Fig. 2), and we test whether this system undergoes a Neel ordering transition when reaching the isotropic limit. This approach is very close in spirit to the one previously done by Chandra and Douçot¹¹ on the J_1 - J_2 square lattice model. This is done within the frame of the linear spin wave theory and the Dyson-Maleev approximation¹². Whereas for the linear spin wave approach there always exists a critical coupling for which the local magnetization is unstable, whatever the value of the spin, in the case of the Dyson-Maleev approach there is a critical coupling only for the case $S = \frac{1}{2}$. The peculiar case $S = \frac{1}{2}$ is explored within a fermionic large- n limit of the $SU(2)$ hamiltonian. It is found that the system should order in a valence bond solid of disconnected 4-spins singlets. The notations, the hamiltonian, and the linear spin wave analysis are introduced in Sec. II. The Dyson-Maleev formalism is shortly described in Sec. III as it can be seen as an extension

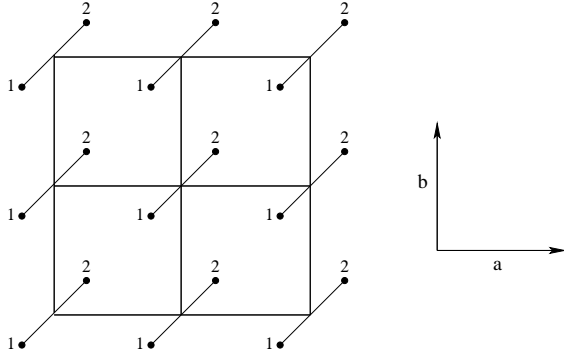
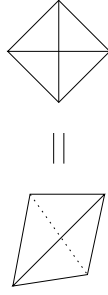
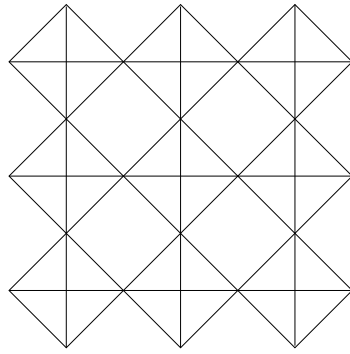


FIG. 1: The checkerboard lattice. It can be pictured as a square lattice of tetrahedra (top). Locally, it reproduces the same environment as the three dimensional pyrochlore lattice. In order to simplify our calculations, it has been described by a square lattice with a 2-spins unit cell (bottom).

of Sec. II. Results of the linear spin wave theory and the Dyson-Maleev approach are presented and discussed in Sec. IV. The case $S = \frac{1}{2}$ is detailed in Sec. V.

II. LATTICE, HAMILTONIAN AND SPIN WAVE ANALYSIS

A. Notations and Lattice Description

The checkerboard lattice can be described as a square lattice with a unit cell containing 2 spins (see Fig. 1). Each cell of the lattice can be obtained from the others by applying the translations $a = (1, 0)$ and $b = (0, 1)$. This means that each site of the lattice can be defined by two indices (i, n) . The first corresponds to the unit cell ($i = 1 \dots N$) where N is the total number of cells in the lattice and the other to the type of the site ($n = 1, 2$). We introduce two kinds of interactions, J and J' . J corresponds to a coupling constant on a square lattice. J' can be seen as a coupling constant within one square over two of the square lattice (see Fig. 2). Using these notations, the Brillouin zone of the underlying Bravais lattice is $\text{BZ}(k_x, k_y) = [-\pi, \pi] \times [-\pi, \pi]$ and the structure coefficients can be defined as :

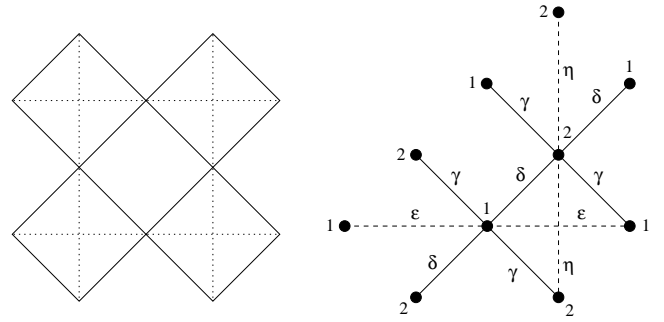


FIG. 2: (left) Lattice of coupling constants J and J' . Bold lines design constant J while dotted lines describe constant J' . (right) Local environment of a unit cell. $\vec{\delta}$ and $\vec{\gamma}$ are related to J -like coupling while $\vec{\epsilon}$ and $\vec{\eta}$ correspond to J' .

$$\begin{aligned} \delta &= \cos(\vec{k} \cdot \vec{\delta}) & \gamma &= \cos(\vec{k} \cdot \vec{\gamma}) \\ &= \cos\left(\frac{k_x + k_y}{2}\right) & &= \cos\left(\frac{k_x - k_y}{2}\right) \\ \epsilon &= \cos(\vec{k} \cdot \vec{\epsilon}) & \eta &= \cos(\vec{k} \cdot \vec{\eta}) \\ &= \cos(k_x) & &= \cos(k_y) \end{aligned} \quad (1)$$

where $\vec{\delta}$, $\vec{\gamma}$, $\vec{\epsilon}$ and $\vec{\eta}$ are depicted in Fig. 2.

B. Spin Wave Hamiltonian

The Heisenberg hamiltonian for this system is

$$H = - \sum_{ij} J_{ij} S_i \cdot S_j \quad (2)$$

where J_{ij} are coupling constants ($J_{ij} < 0$ for an antiferromagnet) and S_i is the spin located at site i . Using the previous notation, the hamiltonian can be written

$$\begin{aligned} H &= -\frac{J}{2} \sum_{i=1}^N \sum_{\vec{\delta}} S_i^1 \cdot S_{i+\vec{\delta}}^2 - \frac{J}{2} \sum_{i=1}^N \sum_{\vec{\delta}} S_i^2 \cdot S_{i+\vec{\delta}}^1 \\ &\quad - \frac{J}{2} \sum_{i=1}^N \sum_{\vec{\gamma}} S_i^1 \cdot S_{i+\vec{\gamma}}^2 - \frac{J}{2} \sum_{i=1}^N \sum_{\vec{\gamma}} S_i^2 \cdot S_{i+\vec{\gamma}}^1 \\ &\quad - \frac{J'}{2} \sum_{i=1}^N \sum_{\vec{\eta}} S_i^2 \cdot S_{i+\vec{\eta}}^2 - \frac{J'}{2} \sum_{i=1}^N \sum_{\vec{\epsilon}} S_i^1 \cdot S_{i+\vec{\epsilon}}^1 \end{aligned} \quad (3)$$

where the sum is performed over the N unit cells, i.e it involves $2N$ sites. In our notation, $S_i^u \cdot S_{i+\vec{t}}^v$ means “the site of type v that can be reached from the site u of unit cell i making translation \vec{t} ”. This spin hamiltonian may be transformed into a boson hamiltonian through

an Holstein-Primakoff transformation, provided that we know its Mean Field ground states (MF) from the square lattice limit to the checkerboard lattice limit, i.e for all values of $r = J'/J$. One way to know the MF ground state(s) is to compute the Fourier transform of the interactions on the lattice¹³.

$$H = - \sum_{i,j} J_{ij} S_i \cdot S_j = \sum_{\vec{q}} J(\vec{q}) S_{\vec{q}} \cdot S_{-\vec{q}} \quad (4)$$

As we here deal with a 2-spin unit cell, its Fourier transform $J(\vec{q})$ is a 2×2 matrix and must be diagonalized to find the normal modes $\lambda^{\mu=1,2}(\vec{q})$. The ground state (if unique) then corresponds to the lowest eigenvalue $\lambda^1(\vec{q}_0)$ and is described by the propagation vector \vec{q}_0 and the associated eigenvector $V_1(\vec{q}_0)$ which fixes the inner structure of the unit cell. In the range $0 \leq r < 1$, \vec{q}_0 always equals 0 and the eigenvector is always equal to $(1, -1)$ which means that the ground state is non-degenerate and corresponds to the antiferromagnetic Néel state (see Fig. 3 top and middle). At the peculiar point $r = 1$, we obtain a flat branch, signaling that at the MF level, the system is continuously degenerate (see Fig. 3 bottom), as previously noted in Ref. 13. That behavior can be explained in terms of local degrees of freedom. In the limit $J' = J$, we note that the hamiltonian may be decomposed as a sum of squares over “tetrahedra”, as it has been done in the kagomé as well as in the pyrochlore lattice

$$\begin{aligned} H &= -J \sum_{ij} S_i \cdot S_j \\ &= -\frac{J}{2} \sum_{\text{Tet.}} \left(\sum_{i=1}^4 S_i \right)^2 + 2NJS(S+1) \end{aligned} \quad (5)$$

We see that the classical ground state is defined by the constraint $\sum_{i=1}^4 S_i = 0$ on each tetrahedron. Furthermore, as tetrahedra are corner sharing, this constraint is not sufficient to order the system and there are an infinite number of ways to satisfy it, which results in a flat branch over the whole Brillouin zone. This is exactly the same phenomenon that was previously observed on the kagomé as well as on the pyrochlore lattice. Nevertheless, the Néel state belongs to this infinite set of MF ground states, and as it is the correct one for any $r < 1$, we will also consider this state by continuity for the point $r = 1$. For the parameter range $r > 1$, the situation is quite different as MF ground states are continuously degenerate along lines corresponding to the border of the square lattice Brillouin zone (see Fig. 4). This precludes a description via a spin wave analysis in this range as no magnetic ground state can be chosen as a trial state. This is the same situation as the one encountered on the kagomé or the pyrochlore lattices where spin wave calculations can only compare relative stability of Néel states without considering the entire set of these states¹⁴. So, we will restrict ourselves to the range $0 \leq r \leq 1$, and consider the antiferromagnetic Néel state as the trial state.

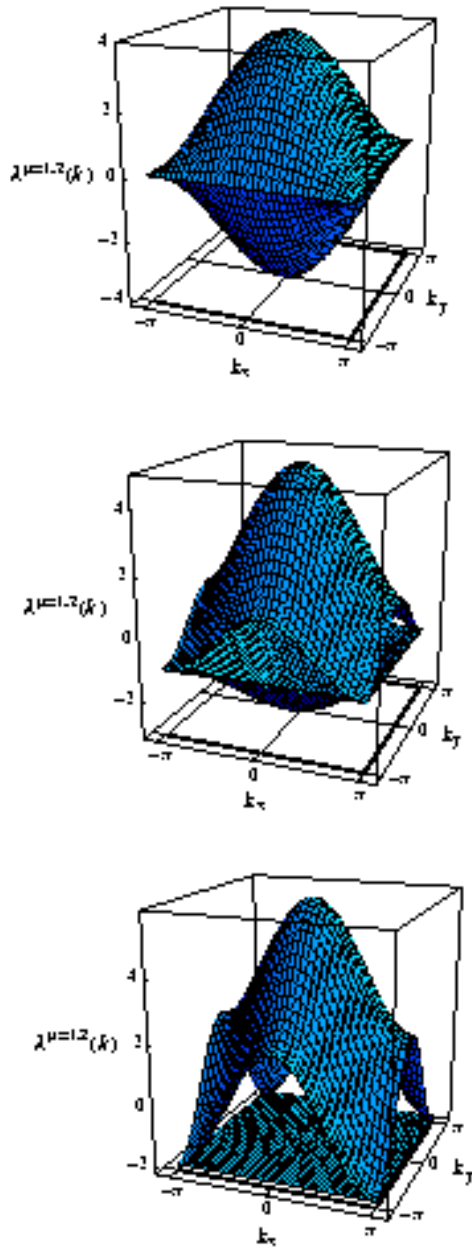


FIG. 3: Fourier transform of the interactions for the square lattice limit ($r = 0$, top), an intermediate case ($r = 0.5$, middle) and the checkerboard limit ($r = 1$, bottom). Each manifold corresponds to an eigenvalue of $J(\vec{q})$.

We therefore introduce two species of bosons, each one related to a different sublattice, and restrict the development of spin operators to the lowest order in the spin wave expansion

$$S_i^{1z} = S - c_i^+ c_i; S_i^{1+} = \sqrt{2S} c_i; S_i^{1-} = \sqrt{2S} c_i^+ \quad (6)$$

$$S_i^{2z} = -S + d_i^+ d_i; S_i^{2+} = \sqrt{2S} d_i^+; S_i^{2-} = \sqrt{2S} d_i \quad (7)$$

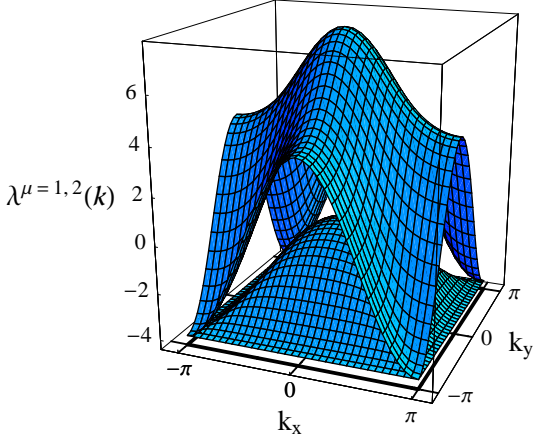


FIG. 4: Fourier transform of the interactions for $r = 2$. Each manifold corresponds to an eigenvalue of $J(\vec{q})$. The mean field ground state is continuously degenerate along lines which enable the choice of a trial ground state for the spin wave analysis.

which allows, after a Fourier transformation, the hamiltonian to be written as follows

$$H = 4NJS^2 - 2NJ'S^2 - 2JS \sum_k f_k c_k^+ c_k + g_k d_k^+ d_k + h_k (c_k d_{-k} + c_k^+ d_{-k}^+) \quad (8)$$

where $f_k = 2 + r(\epsilon - 1)$, $g_k = 2 + r(\eta - 1)$, $h_k = \delta + \gamma$ and $r = J'/J$. δ , γ , ϵ and η are defined according to Eq. 1. Application of a Bogoliubov transformation on this hamiltonian allows it to be written in terms of normal modes, i.e non interacting bosons. The new bosonic operators are α and β and are defined by

$$\alpha = u_\alpha c + v_\alpha d^+ \quad \text{and} \quad \beta = u_\beta d + v_\beta c^+ \quad (9)$$

where (u, v) are real functions of wave vector \vec{k}

$$u_\alpha = \frac{h}{\sqrt{h^2 - (\epsilon_\alpha - f)^2}} \quad v_\alpha = \frac{f - \epsilon_\alpha}{\sqrt{h^2 - (\epsilon_\alpha + f)^2}} \quad (10)$$

$$u_\beta = \frac{\epsilon_\beta + f}{\sqrt{(\epsilon_\beta + f)^2 - h^2}} \quad v_\beta = \frac{h}{\sqrt{(\epsilon_\beta + f)^2 - h^2}}$$

ϵ_α and ϵ_β are two branches of “magnons” and are given by

$$\epsilon_\alpha = \frac{1}{2}(f - g + \sqrt{(f + g)^2 - 4h^2})$$

$$\epsilon_\beta = \frac{1}{2}(-f - g + \sqrt{(f + g)^2 - 4h^2}) \quad (11)$$

This transformation is well defined, i.e $[\alpha_k, \alpha_{k'}^+] = [\beta_k, \beta_{k'}^+] = \delta_{kk'}$ and $[\alpha_k, \alpha_{k'}] = [\alpha_k, \beta_{k'}] = [\alpha_k, \beta_{k'}^+] = 0$. Through this transformation, the hamiltonian now reads

$$H = 4NJS^2 - 2NJ'S^2 - 2JS \sum_k [\epsilon_\alpha(k) \alpha_k^+ \alpha_k + \epsilon_\beta(k) \beta_k^+ \beta_k + \mathcal{C}_k] \quad (12)$$

with

$$\mathcal{C}_k = \frac{1}{2}(\epsilon_\alpha + \epsilon_\beta + (f - g)(u_\alpha^2 - u_\beta^2) - (f + g)) \quad (13)$$

We now restrict ourselves to the ground state, i.e where expectation values are

$$\langle \alpha_k^+ \alpha_k \rangle_o = \langle \beta_k^+ \beta_k \rangle_o = 0 \quad \text{and} \quad \langle \alpha_k \alpha_k^+ \rangle_o = \langle \beta_k \beta_k^+ \rangle_o = 1 \quad (14)$$

This allows the computation of the energy per site in addition to the local magnetization

$$E = \frac{1}{2N} H = 2JS^2 - J'S^2 - JS \sum_{\vec{k}} \mathcal{C}(\vec{k}) \quad (15)$$

$$M = \langle S_i^{1z} \rangle_o = S - \langle c_i^+ c_i \rangle_o = S - \frac{1}{N} \sum_{\vec{k}} v_\alpha^2(\vec{k}) \quad (16)$$

III. DYSON-MALEEV REPRESENTATION

We use the same hamiltonian of Eq. 2 and introduce the Dyson-Maleev transformation¹²,

$$S_i^{1z} = S - a_i^+ a_i \quad ; \quad S_i^{1+} = (2S - a_i^+ a_i) a_i$$

$$S_i^{1-} = a_i \quad (17)$$

$$S_j^{2z} = -S + b_j^+ b_j \quad ; \quad S_j^{2+} = b_j^+ (2S - b_j^+ b_j)$$

$$S_j^{2-} = b_j \quad (18)$$

Because of its algebra, the Dyson-Maleev transformation rewrites the hamiltonian of Eq. 2 as a sum of two and four operators terms. The simplest method to solve the problem is to decouple the four operators term introducing an *a priori* decoupling scheme. In the present case, we follow the mean field decoupling of Ref. 15. Three quantities are introduced that correspond each to a two bosons like excitations,

$$\mathcal{D} = \langle a_i^+ a_i \rangle = \langle b_j^+ b_j \rangle$$

$$\mathcal{O} = \langle a_i^+ a_l \rangle = \langle b_j^+ b_m \rangle \quad ; \quad i \neq l \quad , \quad j \neq m \quad (19)$$

$$\mathcal{T} = \langle a_i^+ b_j^+ \rangle$$

Other types of excitations are neglected and considered as higher energy processes as previously proposed by Takahashi¹⁶,

$$\langle a_i a_i \rangle = \langle b_j^+ b_j^+ \rangle = 0 ; \quad \langle a_i^+ b_j \rangle = \langle a_i b_i^+ \rangle = 0 \quad (20)$$

Using these approximations, the Dyson Maleev hamiltonian is then linearized and after Fourier transformation, it is rewritten as

$$\begin{aligned} H = & 4 NJ(S^2 - \frac{1}{2}(\mathcal{D} + \mathcal{O})^2) \\ & - 2 NJ'(S^2 - \frac{1}{2}(\mathcal{D} - \mathcal{T})^2) \\ & - 2 JS \sum_k f'_k c_k^+ c_k + g'_k d_k^+ d_k + h'_k (c_k d_{-k} + c_k^+ d_{-k}^+) \end{aligned} \quad (21)$$

where $f'_k = 2A + rB(\epsilon - 1)$, $g'_k = 2A + rB(\eta - 1)$, $h'_k = A(\delta + \gamma)$ and $A = 1 - \frac{\mathcal{D} + \mathcal{O}}{2S}$ and $B = 1 - \frac{\mathcal{D} - \mathcal{T}}{2S}$. After this decoupling, the obtained hamiltonian has exactly the same structure as the one obtained through the linear spin wave approximation. The discrepancy between the two methods is hidden in the coefficients f' , g' and h' . Thus, it is possible to diagonalize this hamiltonian exactly in the same manner where the new bogoliubov transformation has again the same structure with the new coefficients f' , g' and h' . Finally the three self consistent coefficients at zero temperature are obtained through the three coupled relations,

$$\begin{aligned} \mathcal{D} &= \frac{1}{N} \sum_k v_\alpha'^2(k) \\ \mathcal{O} &= -\frac{1}{2N} \sum_k u_\alpha'(k) v_\alpha'(k) (\delta + \gamma) \\ \mathcal{T} &= \frac{1}{2N} \sum_k v_\alpha'^2(k) (\epsilon + \eta) \end{aligned} \quad (22)$$

and the local magnetization of the Néel state is simply $M = \langle S_i^{1z} \rangle_0 = S - \mathcal{D}$.

IV. RESULTS OF THE SPIN WAVE APPROACH

In the following, we fix $J = -1$ and take $-1 \leq J' \leq 0$. We first discuss the linear spin wave results and then the Dyson-Maleev approach. Switching to the continuous formulation by use of the correspondance when $N \rightarrow \infty$

$$\frac{1}{N} \sum_{\vec{k}} \longleftrightarrow \frac{1}{v_0} \int_{BZ} d^2 \vec{k} \quad (23)$$

where v_0 is the volume of the Brillouin zone (BZ), Eq. 15 and Eq. 16 become

$$E = 2JS^2 - J'S^2 - \frac{JS}{4\pi^2} \int_{BZ} C(\vec{k}) d^2 \vec{k} \quad (24)$$

$$M = S - \frac{1}{4\pi^2} JS \int_{BZ} v_\alpha^2(\vec{k}) d^2 \vec{k} \quad (25)$$

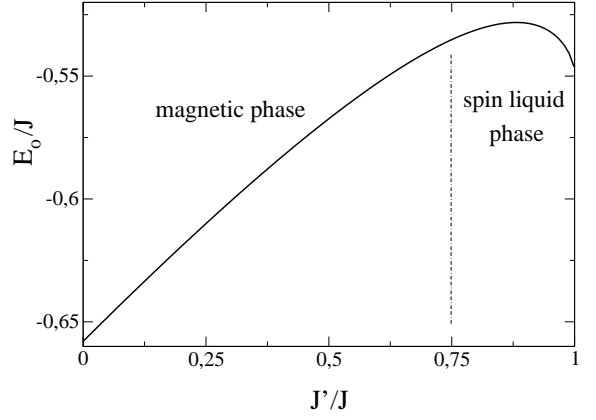


FIG. 5: Energy per site as a function of the ratio $r = J'/J$, i.e between the limits of the square lattice and the checkerboard lattice, for $S = 1/2$. Beyond the critical ratio $r \approx 0.75$, the value of the energy is meaningless as it describes the energy of an unstable state.

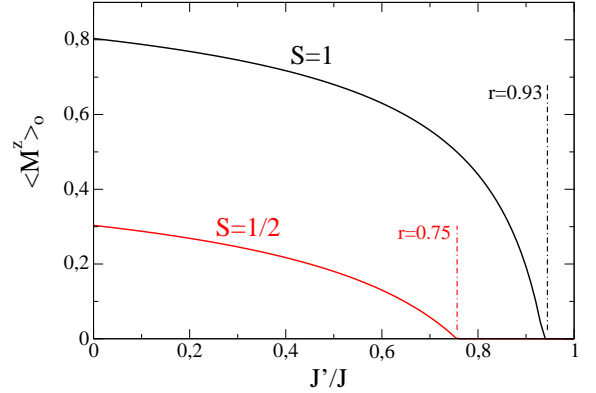


FIG. 6: Local magnetization as a function of the ratio $r = J'/J$, i.e from the square lattice to the checkerboard lattice. Red lines correspond to the calculations made for $S = 1/2$ and black lines for $S = 1$.

In Fig. 5 and 6 both quantities are plotted as functions of the ratio $r = J'/J$. For the case $r = 0$, well known results for the $S = 1/2$ square lattice are recovered : $E = -0.658$ and $M = 0.3$. The magnon spectrum is very simple; there is only one dispersive branch, which is two times degenerate in our case because of the 2-spin unit cell description (Fig. 7 top). With increasing r , there are three zones to distinguish. First, in the range $0 \leq r \leq r_c$, the magnon spectrum has two distinct manifolds, each of these being dispersive (Fig. 7 middle). This occurs now because the site of the unit cell no longer have the same symmetry. r_c corresponds to a critical coupling below which the local magnetization is finite, even renormalized by quantum corrections. For $S = 1/2$, $r_c \approx 0.75$ which was already obtained in Ref. 17 and for $S = 1$, $r_c \approx 0.93$. Critical values for higher spins are shown in the phase diagram of Fig. 8.

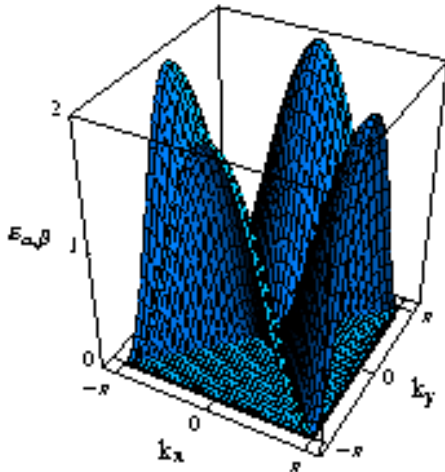
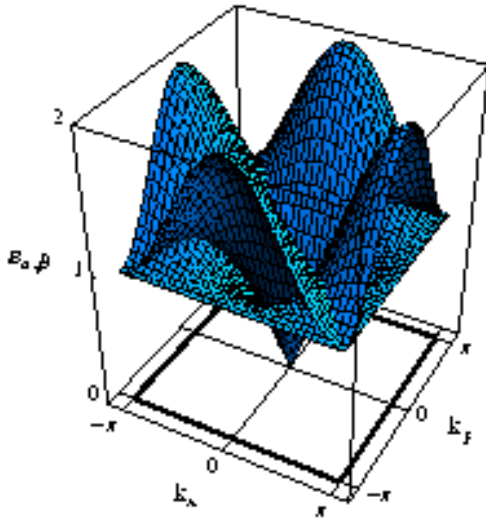
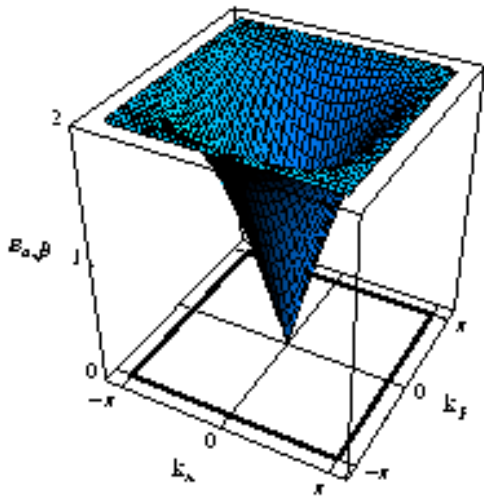


FIG. 7: Magnons dispersions $\epsilon_{\alpha,\beta}(k)$ over the Brillouin zone. From top to bottom, $r = 0, 0.5, 1$. At $r = 1$, the lowest branch is non-dispersive. This means that this point is remarkable and reveals (as in the kagomé and the pyrochlore lattice case) the presence of a soft mode related to local degrees of freedom.

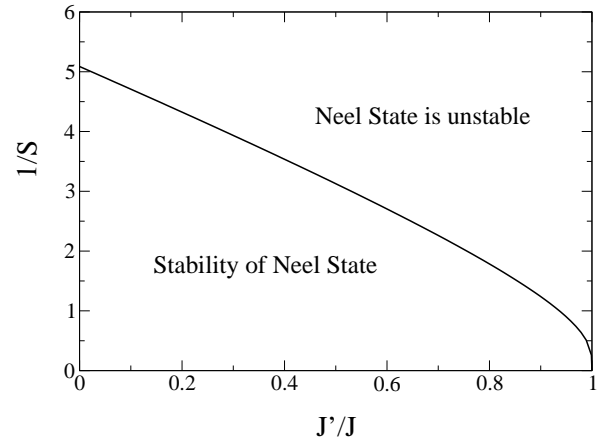


FIG. 8: Stability of the Neel state. The straight line indicates the threshold below which the Neel state is stable for a given ratio $r = J'/J$. Over this line, it is destabilized by geometry and quantum fluctuations. For $r = 1$, it is always unstable, whatever the value of the spin S .

The second zone corresponds to the range $r_c \leq r < 1$. Because of quantum corrections, local magnetization is renormalized to zero, which means that in this approximation, the system does not show magnetic ordering. Even if quantum fluctuations drive the system to disorder, one notes that magnons are still dispersive. This means that there is no peculiar contribution coming from their structure. This is no longer the case for the special point $r = 1$. At this point, the lowest branch of spin waves is flat over the whole Brillouin zone (Fig. 7 bottom). This has several consequences. First, this means that at the level of this approximation, there will always be a critical coupling, whatever the value of the spin. This comes directly from the non-analytic behavior of $v_\alpha(\vec{k})$ when $r \rightarrow 1$ along directions $ky = \pm kx$. Because of that the local magnetization diverges as $-1/\sqrt{1-r}$, i.e. is renormalized to zero, whatever the value of S . Consequently, we obtain a phase diagram $(1/S, J'/J)$ very similar to the one of the $J_1 - J_2$ square lattice model where J'/J plays the role of J_2/J_1 (see Fig. 8 and Fig. 2 of Ref. 11). This problem of flat mode is often encountered in frustrated lattices and it rules out the possibility of studying the $r = 1$ point without going to next order of expansion in our model, i.e. without including quartic terms. Whether such an inclusion of quartic terms is relevant is not clear as it corresponds to consider quartic modes as perturbations of *zero* quadratic modes. Nevertheless, it is the simplest next step to be done in the frame of spin wave (Holstein-Primakoff) analysis¹⁴. Second, it has a meaning very close to MF conclusions. If the lowest branch of magnons is flat, this means that the system has no spin stiffness. Thus, any local deformation will not propagate through lattice. This is very close to the argument of continuous degeneracy obtained through the MF approach, i.e. the existence of an infinite number of local degrees of freedom (see Eq. 5). These degrees

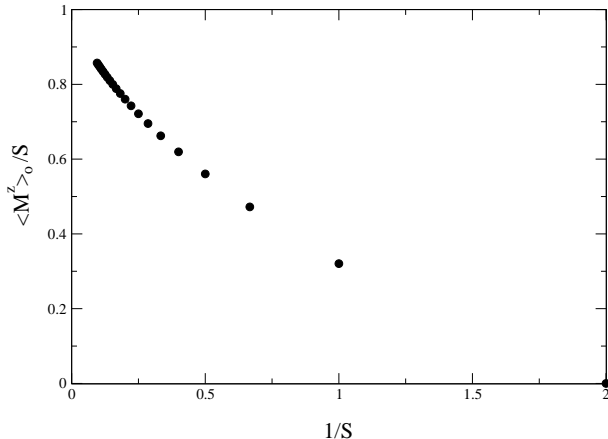


FIG. 9: Relative local magnetization of the Néel state versus the inverse spin value $1/S$ at the isotropic point. For all $S \geq 1$, the local magnetization is finite, suggesting that the ground state could be the Néel state. For $S = 1/2$, the local magnetization is renormalized to zero by quantum fluctuations.

of freedom are one of the signatures of frustrated systems and may be counted, in the case of classical spins, through the “Maxwellian counting” rule⁷. At the level of the LSW approximation, this means that quantum fluctuations and geometrical frustration may destabilize the Néel state for a finite range of J' . Whether a quantum spin liquid ground state in this range is stable is beyond this approach even if the existence of critical couplings goes in the right direction.

We now turn to the Dyson-Maleev approach. As for the preceding case, the local magnetization has been computed for different values of the spin. The main result is that for all $S \geq 1$, there is no critical coupling, i.e. the local magnetization of the Néel state is always finite in the isotropic limit $r = 1$. This is illustrated in Fig. 9 where reduced local magnetization $\langle S_i^z \rangle_0 / S$ is plotted versus the inverse spin value $1/S$ at $r \rightarrow 1$. The only exception is for $S = \frac{1}{2}$ for which it seems that there is a critical coupling at $r \approx 0.98$. To test whether the stability of the Néel state for the $S = \frac{1}{2}$ comes from a flat mode or from quantum fluctuations, we have plotted the associated dispersions over the whole Brillouin zone (see Fig. 10). From the structure of the bosons excitations, it is clear that including quantum fluctuations via the Dyson-Maleev formalism destroys the pathological structure of the flat mode. Therefore, destabilization of the Néel state is only driven by quantum fluctuations within this approximation and not by a zero spin stiffness as it was the case in the LSW approximation in the limit $r \rightarrow 1$.

These results are quite surprising as they are qualitatively different from the LSW approximation. This suggests that the more accurately the quantum fluctu-

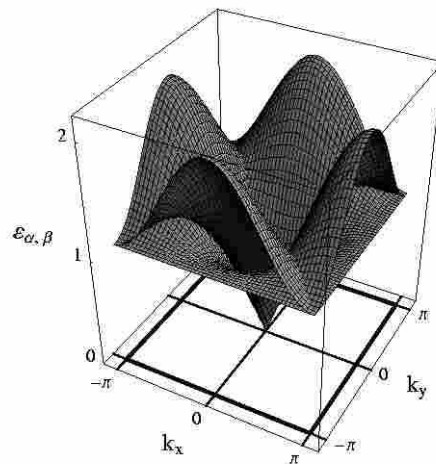


FIG. 10: Energy dispersions corresponding to the bosons excitations around the Néel state for the $S = 1/2$ case in the limit $r \rightarrow 1$. The dispersions are no longer pathological as they are in the LSW approximation and the flat mode is destroyed. This clearly indicates that destabilization of the Néel state is driven here only by quantum fluctuations.

ations are taken into account, the more the Néel state is stable, even in the isotropic limit. This is unexpected as the checkerboard antiferromagnet was expected to behave like the kagomé antiferromagnet. In the latter case, the reduction of the local magnetization to zero by quantum fluctuations and geometry, within a finite range of couplings, has been shown using two distinct numerical methods¹⁸. It was found that going from the triangular limit to the kagomé limit, there is a singular point associated to a critical coupling ($r_c = J'_c / J \approx 0.9$), where local magnetization vanishes. Here, we obtain the same conclusion within the LSW approximation but not within the mean field treatment of the Dyson-Maleev approach. Whether this discrepancy comes from the quantum fluctuations that are better incorporated in the latter formalism, or comes from the mean field treatment of the DM representation is not clear. Nevertheless, it is interesting to note that a recent work¹⁹ shows the same tendency, i.e. a transition from an $S = 0$ ground state to a stable Néel state with increasing spin size S . If the present calculations treat correctly quantum fluctuations (which is not proven in this paper), the frontier between the expected VBS state and the Néel ordering¹⁹ would then be at $S = 1$. Nevertheless, it should be stressed that the present work does not test whether other classical ground states could be stable at the isotropic point and have the same or a different energy than the Néel ground state. Consequently, an intrinsic or accidental degeneracy of magnetic ground states for $S \geq 1$ is not ruled out by this approach.

V. THE $S = 1/2$ CASE

As shown in the preceding sections, it seems that only for $S = 1/2$ can the ground state be non-magnetic. To shed light on the behavior of the $S = 1/2$ checkerboard antiferromagnet, it is possible to use a “fermionic” $SU(n)$ generalization of the $SU(2)$ group [Note that $n > 2$ does not correspond to a higher spin representation of $SU(2)$]. Therefore, a mean-field solution of the $SU(n)$ hamiltonian is expected to be much closer to the $SU(2)$ physics than the classical description of sec. II B]. This formalism has been previously introduced by Marston and Affleck²⁰ and applied to the square antiferromagnet. The advantage of this description is that it works on all lattices, even frustrated²¹ or not bipartite, and that it is well suited for the checkerboard antiferromagnet as spin order never occurs in the exactly solvable large- n limit²⁰, as it is expected in the range $r_c \leq r \leq 1$ for $n = 2$. At large n , the hamiltonian can be written as

$$H = \sum_{(i,j)} \left\{ \left(\frac{n}{J} \right) |\chi_{ij}|^2 + \sum_{\alpha=1}^n (\chi_{ij} c_{i\alpha}^+ c_{j\alpha} + \text{H.c}) \right\} \quad (26)$$

where $\chi_{ij} = (J/n)c_{i\alpha}^+ c_{j\alpha}$ are bond variables and where spin-spin interaction has been expressed by use of electron operators through $S_i \cdot S_j = (1/2) \sum_{\alpha,\beta} c_{i\alpha}^+ c_{j\beta}^+ c_{j\beta} c_{i\alpha} + \text{constant}$. The χ variables may be seen as valence bond operators²² as $(n/J)\chi_{ij}^+ \chi_{ij}$ is the number of valence bonds on the link (ij) . Therefore, in this formalism, every ground state is described by a map of these complex scalar fields. Several authors have concentrated on the mean-field solutions (“ $1/n = 0$ ”)^{20,23,24} and in particular, it is possible to apply here a theorem established by D. Rokhsar²⁴. First it is clear that the checkerboard antiferromagnet is “dimerizable with respect to J ” as “it is possible to partition the network into disjoint pairs of sites such that (a) every site belongs to one and only one pair, and (b) for each pair (i,j) we have $J_{ij} = J$ ”. In the range $J \geq J'$ it is possible to apply his theorem which shows that mean-field ground states are (spin-Peierls or box)-phases²⁴ (see Fig. 11). Keeping in mind that the case of interest is for $n = 2$, we look for the proposed states that lower the energy of the real $S = 1/2$ case. It is straightforward to see that box-phases lower this energy with respect to J , as soon as these phases are regular tilings of the underlying square lattice by disconnected J -squares (see Fig. 11). Taking now into account the J' couplings, only one of these phases survives, where J' links are not frustrated. At this point, it means that *if* the $SU(n)$ description of the $SU(2)$ case is relevant, it suggests that for $S = 1/2$, in the range $r_c \leq r \leq 1$, the ground state should be two times degenerate (because there are two choices for the tiling), consisting in a valence bond solid of disconnected squares without crossings (in the range $0 \leq r < r_c$ it is clear that this formalism is not relevant as the local magnetisation is finite). The proposed ground state

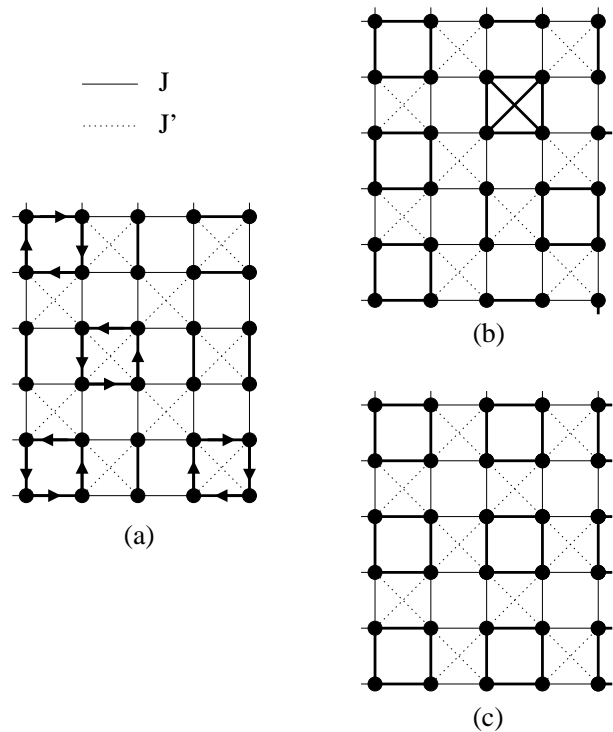


FIG. 11: (a) General box phase on the J square lattice of the anisotropic checkerboard antiferromagnet (as shown in Fig. 4 of Ref. 24). Bold lines without arrows correspond to non zero χ_{ij} while thin lines, plain or dashed, correspond to $\chi_{ij} = 0$. Bold lines with arrows indicate that $\chi_{ij} = \chi e^{i\pi/4}$ where χ is real. The product of χ_{ij} around each box is negative, indicating a flux of π . These boxes are the large- n equivalent of a 4-spins singlet on a square. (b) Picture of a general box phase for the $S = 1/2$ case. Bold squares correspond to 4-spins singlets and bold lines to 2-spins singlets. If J' interactions are within a box, they must be taken into account and are also in bold as they enter the calculation of the energy. The different energies for squares with crossings, squares without crossings and links are respectively $E = -1.5$, $E = -2$ and $E = -0.75$. (c) Picture of the valence bond solid for the $S = 1/2$ case, expected to be the ground state. This state is two times degenerate and involves only squares without crossings.

(see Fig. 11(c)) could be tested by comparing the VBS energy per site $E = -0.5$ and the correlations functions with results of exact diagonalisations for example²⁵.

VI. DISCUSSION AND CONCLUSION

To conclude, Linear Spin Wave analysis has shown that away from the isotropic checkerboard lattice limit, there is a finite range of coupling for which the Néel state is unstable, whatever the value of the spin. Strikingly, when using a self consistent decoupling within the Dyson-Maleev formalism, it is shown that the Néel state is never destabilized, excepted for the $S = \frac{1}{2}$ case. The stability of the Néel state with respect to other magnetized states has not been tested in this work. Recent

work¹⁹ supports that this state should be the ground state for large S . It is compatible with the present results although it is at variance with results obtained with the infinite-component²⁶ antiferromagnetic model on the checkerboard lattice ($d \rightarrow \infty$). A possible explanation for this²⁷ is that for large S , there should be quantum order by disorder (as supported in¹⁹) but this order by disorder comes with an energy scale of J/S rather than J . Therefore, in the classical limit, the temperature at which the correlation length grows exponentially goes to zero. In other words, the limits $T \rightarrow 0$ and $S \rightarrow \infty$ (or $d \rightarrow \infty$) should not commute. For the special $S = \frac{1}{2}$ case, the fermionic large- n limit suggests that the ground state is a valence bond solid of disconnected 4-spins singlets on squares without crossings. That conclusion is consistent with results of Refs. 19 and 25.

The present work shows that the isotropic checkerboard antiferromagnet should display behaviors quali-

tatively different from the one of the kagomé and the pyrochlore antiferromagnet. Moreover, quantum fluctuations have to be treated with care as they can drive the system from a purely quantum ground state to a Néel like ground state. In this frame, the structure of the singlet and triplet towers of state should be extremely S -dependent and exact diagonalization of finite clusters with different spin size would be of high interest, especially to test whether the discrepancy already appears between the $S = \frac{1}{2}$ and the $S = 1$ cases.

Acknowledgments

The author would like to thank Maged Elhajal, Peter Holdsworth, Claudine Lacroix and Roderich Moessner for interesting and stimulating discussions.

-
- * Electronic address: canals@polycnrs-gre.fr; URL: <http://ln-w3.polycnrs-gre.fr/pageperso/canals/>
- ¹ F. D. M. Haldane, Phys. Lett. A **93**, 464 (1983).
 - ² G. H. Wannier, Phys. Rev. **79**, 357 (1950).
 - ³ R. M. F. Houtappel, Physica **16**, 425 (1950).
 - ⁴ E. H. Lieb and D. Mattis, J. Math. Phys. (N.Y.) **3**, 749 (1962).
 - ⁵ P. Lecheminant, B. Bernu, C. Lhuillier, L. Pierre and P. Sindzingre, Phys. Rev. B **56**, 2521 (1997).
 - ⁶ D. A. Garanin and B. Canals, Phys. Rev. B **59**, 443 (1999).
 - ⁷ R. Moessner and J. T. Chalker, Phys. Rev. Lett. **80**, 2929 (1998); R. Moessner and J. T. Chalker, Phys. Rev. B **58**, 12049 (1998). R. Moessner, *D. Phil. thesis* (Oxford University, 1996)
 - ⁸ B. Canals and C. Lacroix, Phys. Rev. Lett. **80**, 2933 (1998); B. Canals and C. Lacroix, Phys. Rev. B **61**, 1149 (2000).
 - ⁹ For a collection of articles, see *Magnetic systems with Competing Interactions : Frustrated Spin System*, edited by H. T. Diep (World Scientific, Singapore, 1994); for Ising systems, see R. Liebmann, *Statistical Mechanics of Periodic Frustrated Ising Systems* (Springer, Berlin, 1986); for reviews, see A. P. Ramirez, Annu. Rev. Mater. Sci. **24**, 453, (1994); P. Schiffer and A. P. Ramirez, Comments Cond. Mat. Phys. **18**, 21, (1996); M. J. Harris and M. P. Zinkin, Mod. Phys. Lett. B **10**, 417, (1996).
 - ¹⁰ E. H. Lieb and P. Schupp, Phys. Rev. Lett. **83**, 5362 (1999).
 - ¹¹ P. Chandra and B. Douçot, Phys. Rev. B **38**, 9335 (1988).
 - ¹² F. J. Dyson, Phys. Rev. **102**, 1217 (1956); F. J. Dyson, Phys. Rev. **102**, 1230 (1956); S. V. Maleev, Zh. Eksp. Teor. Fiz. **30**, 1010 (1957) [Sov. Phys. JETP **6**, 776 (1958)].
 - ¹³ J. N. Reimers, A. J. Berlinsky and A.-C. Shi., Phys. Rev. B **43** (1991) 865.
 - ¹⁴ A. Chubukov, Phys. Rev. Lett. **69**, 832 (1992).
 - ¹⁵ D. Chu and J. L. Shen, Phys. Rev. B **44**, 4689 (1991).
 - ¹⁶ M. Takahashi, Phys. Rev. B **40**, 2494 (1989).
 - ¹⁷ R.R.P.Singh, O.A.Starykh and P.J.Freitas, J. Appl. Phys. **83**, 7387 (1998).
 - ¹⁸ D. J. J. Farnell, R. F. Bishop and K. A. Gernoth, cond-mat/0010477. C. Waldtmann, P. Lecheminant, *unpublished*.
 - ¹⁹ R. Moessner, Oleg Tchernyshyov and S. L. Sondhi, cond-mat/0106288.
 - ²⁰ J. B. Marston and I. Affleck, Phys. Rev. B **39**, 11538 (1989).
 - ²¹ J. B. Marston and C. Zeng, J. Appl. Phys. **69**, 5962 (1991).
 - ²² Ian Affleck and J. Brad Marston, Phys. Rev. B **37**, 3774 (1988).
 - ²³ Thierry Dombre and Gabriel Kotliar, Phys. Rev. B **39**, 855 (1989).
 - ²⁴ Daniel S. Rokhsar, Phys. Rev. B **42**, 2526 (1990).
 - ²⁵ J.-B. Fouet, M. Mambrini, P. Sindzingre and C. Lhuillier, condmat/0108070.
 - ²⁶ B. Canals and D. A. Garanin, cond-mat/0102235.
 - ²⁷ R. Moessner, private communication.